IOPscience iopscience.iop.org

Home Search Collections Journals About Contact us My IOPscience

Quantization effects on the phonon-limited electron mobility in ultrathin SOI, sSOI and GeOI devices

This article has been downloaded from IOPscience. Please scroll down to see the full text article.

2007 Semicond. Sci. Technol. 22 413

(http://iopscience.iop.org/0268-1242/22/4/021)

View the table of contents for this issue, or go to the journal homepage for more

Download details:
IP Address: 129.8.242.67
The article was downloaded on 18/06/2010 at 10:47

Please note that terms and conditions apply.

IOP Publishing — Semiconductor Science and Technology

Semicond. Sci. Technol. **22** (2007) 413–417 doi:10.1088/0268-1242/22/4/021

Quantization effects on the phonon-limited electron mobility in ultrathin SOI, sSOI and GeOI devices

S Barraud

CEA-DRT-LETI-Minatec/D2NT/LSCDP, 17 rue des Martyrs, 38059 Grenoble, France

E-mail: sylvain.barraud@cea.fr

Received 25 October 2006, in final form 23 January 2007
Published 19 March 2007
Online at stacks.iop.org/SST/22/413

Abstract
The phonon-limited electron mobility in inversion layers is studied in fully depleted silicon-on-insulator (FD-SOI) MOSFET as a function of transverse effective field and semiconductor film thickness. A quantum-mechanical procedure based on the solution of 1D-coupled Poisson/Schrödinger equations is employed to calculate the phonon–electron mobility using a relaxation time approximation. The influence of quantization effects on the phonon-limited electron mobility in ultrathin SOI, strained-SOI and GeOI MOSFET is investigated. A comparative study of mobility shows an enhancement factor varying from 1.5 to 2.5 for film thicknesses ranging from 5 nm to 20 nm using both strained-silicon and germanium materials.

1. Introduction

To pursue towards the continuing improvement of performances and density of ULSI technology, MOSFET devices are scaled down to sub-50 nm dimensions. The downscaling of conventional bulk MOSFET into the nanometre regime faces several well-known challenges such as the control of short channel effect (SCE) and a ratio I_{on}/I_{off} which must keep an acceptable value with the decrease of the channel length [1]. Many fundamental limiting factors have been identified in the past to limit the performances of logical and analogue circuits in the conventional bulk MOSFET such as the source-to-drain tunnelling, quantum-mechanical tunnelling through the gate oxide [2, 3]. Moreover, near the limit of scaling there are a decreasing number of the channel impurities whose random distribution leads to significant fluctuations of the threshold voltage and off-state leakage current [4, 5]. To overcome these issues, new materials and new device architectures are currently underway. Fully depleted silicon-on-insulator MOSFET has been recognized as a promising device structure for low power application, because of the steep subthreshold slope and low junction capacitance [6, 7]. Recently Shoji *et al* have studied the phonon-limited electron mobility in these devices [8, 9]. Using a relaxation time approximation method, they have calculated the phonon-limited electron mobility in double-gate silicon-on-insulator devices. They show that in double-gate-nMOSFET, as the silicon thickness is reduced, phonon-limited electron mobility increases to a maximum at T_{SI} of ∼3 nm and decreases monotonically with the reduction of the silicon film thickness. The contribution of surface roughness due to both Si–SiO_2 interfaces and Coulomb interaction has also been studied on electron mobility by Monte Carlo simulation [10]. Another way to improve the carrier mobility consists in using material with high mobility such as strained silicon (sSi) or germanium (Ge). Indeed, under a biaxial tensile strain the electron mobility is enhanced over unstrained silicon. Lauer *et al* have recently demonstrated the fabrication of highly uniform SiGe-free sSOI (strained-Si-on-insulator) wafers with 20% Ge equivalent strain and shown that the enhanced mobility is maintained in strained Si films transferred directly to SiO_2 [11]. Takagi *et al* have investigated the phonon-limited mobility of strained Si MOSFET transistors fabricated on a SiGe substrate through theoretical calculations including quantization effects [12]. They reported that the occupancy of the twofold valleys reaches almost 100% around a Ge content of 20%, where the energy difference between the lowest subbands is sufficiently high compared to the thermal energy. Moreover, they concluded that inter-valley phonon scattering is removed for the Ge content of 20% more and only intravalley acoustic phonon scattering is dominant in the calculated phonon-limited electron mobility.

 © 2007 IOP Publishing Ltd Printed in the UK

In this paper the phonon-limited electron mobility in SOI n-channel MOSFETs is investigated for various semiconductor film thicknesses in Si, sSi and Ge materials using a relaxation time approximation method. After having described the theoretical model we will focus on a comparison of electron mobility in the three devices.

2. Computation method

In this work we use the approach developed by Shoji *et al* where the eigenstates and the wavefunctions are calculated to evaluate the phonon-limited electron mobility. In the calculation the coupled Poisson–Schrödinger equations are solved self-consistently in the semiconductor film. The conduction band of unstrained bulk silicon has six equivalent valleys along the ⟨1 0 0⟩ directions of the Brillouin zone, and the constant energy surface is ellipsoidal with a transverse mass, $m_t = 0.19m_0$ and a longitudinal mass $m_l = 0.916m_0$. In the inversion layer, the six Δ valleys are classified into twofold degenerate valleys with m_l perpendicular to the Si/SiO_2 interface and the fourfold degenerate valleys with m_t perpendicular to the interface. The subbands E_i (named 'unprimed') are associated with the two valleys with m_l perpendicular to the surface and the subbands E_i' (named 'primed') are associated with the four valleys with m_t perpendicular to the surface. In the case of strained silicon there are important effects, such as strain-induced splitting inducing significant changes in the conduction and valence band. The biaxial tensile strain lifts the sixfold degeneracy in the conduction band inducing lowered twofold states Δ_2 (valleys perpendicular to the strain direction) and raised fourfold states Δ_4. The resulting conduction band offset and the energy splitting are dependent of Ge mole fraction in the relaxed $Si_{1-x}Ge_x$ layer. As a result, electrons preferentially occupy the lower energy band (Δ_2 valleys) where the effective mass at 300 K is reduced in comparison with the Si value.

The germanium conduction band consists of four ⟨1 1 1⟩ minima at the edge of the Brillouin zone, a single minimum at the centre of the zone, and six ⟨1 0 0⟩ minima near the zone edge [14]. The ⟨1 1 1⟩ minima have ellipsoidal constant energy surfaces characterized by longitudinal m_l and transverse m_t effective masses. In the ⟨1 1 1⟩ valleys the longitudinal and transverse masses are $1.588m_0$ and $0.08152m_0$, respectively [16].

In table 1 we list the parameters which are required to calculate the phonon-limited electron mobility in the three materials in the crystallographic direction [1 0 0]. The subband energies, the envelope function of the eigenstate and the surface carrier concentration occupying each subband can be calculated by solving the Schrödinger and Poisson equations self-consistently. A description of the Poisson and Schrödinger equations can be found in [17]. The Schrödinger equation for the twofold and the fourfold valleys is simply described by equations (1) and (2),

$$-\frac{\hbar^2}{em_l}\frac{d^2}{dz^2}\psi_i(z) - eV(z)\psi_i(z) = E_i\psi_i(z) \quad (1)$$

$$-\frac{\hbar^2}{em_t}\frac{d^2}{dz^2}\psi_i'(z) - eV(z)\psi_i'(z) = E_i'\psi_i'(z), \quad (2)$$

where $\psi_i(z)$ and E_i are the envelope function and the subband energy in the twofold valleys, $\psi_i'(z)$ and E_i' are the envelope function and the subband energy in the fourfold valleys and $V(z)$ is the potential energy. The momentum-relaxation rate $\tau_{ac}^{ij}(E)$ for deformation potential scattering by intravalley acoustic phonons from the ith subband to the jth subband, is given by [12]

$$\frac{1}{\tau_{ac2}^{ij}(E)} = \frac{n_{v2}^{ac} \times m_{d2} \times D_{ac} \times k_B T}{\hbar^3 \times \rho s_l}\frac{1}{W_{i,j}} \quad (3)$$

$$W_{i,j} = \left(\int \xi_i^2(z)\xi_j^2(z)\,dz\right)^{-1}, \quad (4)$$

where D_{ac} denotes the deformation potential due to the acoustic phonon, n_v^{ac} is the degeneracy of the valley with respect to intravalley scattering, ρ is the mass density of the crystal, and s_l is the longitudinal sound velocity. $W_{i,j}$ is the form factor determined by the wavefunctions of the ith and the jth subbands. Similar equations are used for the fourfold valleys. In the following section only the first subband will be considered for the calculations of the form factor. $W_{i,i}$ is interpreted to be the effective thickness of the wavefunction of the ith subband with respect to z [12].

Table 1. Material parameters in silicon and germanium.

Material	Silicon	Germanium		
m_l	$0.916m_0$	$1.588m_0$		
m_t	$0.191m_0$	$0.0185m_0$		
m_{d2}	$0.191m_0$	$0.2975m_0$		
m_{d4}	$0.417m_0$			
m_{c2}	$0.191m_0$	$0.152m_0$		
m_{c4}	$0.315m_0$			
ρ	2329 kg cm^{-3}	5320 kg cm^{-3}		
s_l	6607 m s^{-1}	5310 m s^{-1}		
D_{ac}	6.6 eV	6.5 eV		
Surface orientation	m_x	m_y	m_z	g_v
Si {1 0 0}	0.19	0.19	0.916	2
	0.19	0.916	0.19	4
Ge {1 0 0}	0.0815	1.0858	0.119	4

3. Phonon-limited mobility

We start the comparative study of phonon-limited electron mobility between SOI, sSOI and GeOI devices by analysing the evolution of the electronic states in an ultrathin silicon film and their influence on the electron mobility. Then, we will compare with other promising materials such as strained silicon and germanium. In all cases the equivalent oxide thickness (EOT) is taken as 2 nm with a channel doping equal to 10^{16} cm^{-3}. Different film thicknesses ranging from 20 nm down to 1 nm were considered. The resolution of the coupled Poisson–Schrödinger equations allows us to follow the evolution of the subband energies for both twofold valleys and fourfold valleys with the electric field defined as

$$E_{eff} = \frac{\int_0^{T_{SOI}} n(z)E(z)\,dz}{\int_0^{T_{SOI}} n(z)\,dz}, \quad (5)$$

$E(z)$ being the local transverse electric field and T_{SOI} the film thickness. The subbands E_i associated with the two valleys

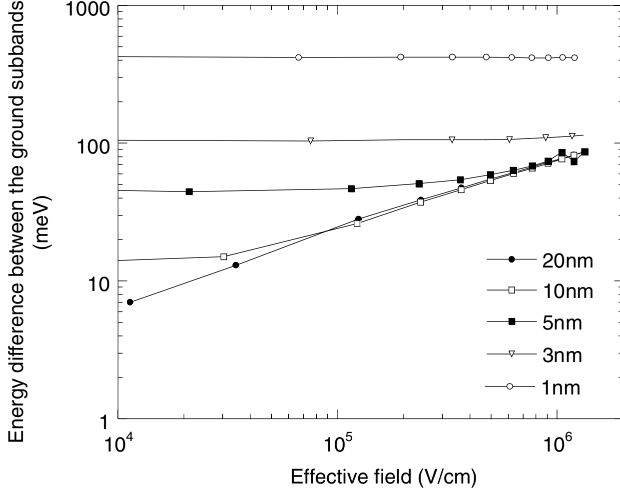

Figure 1. Energy difference between the ground subbands of the unprimed and primed valleys versus the effective field (E'_0–E_0).

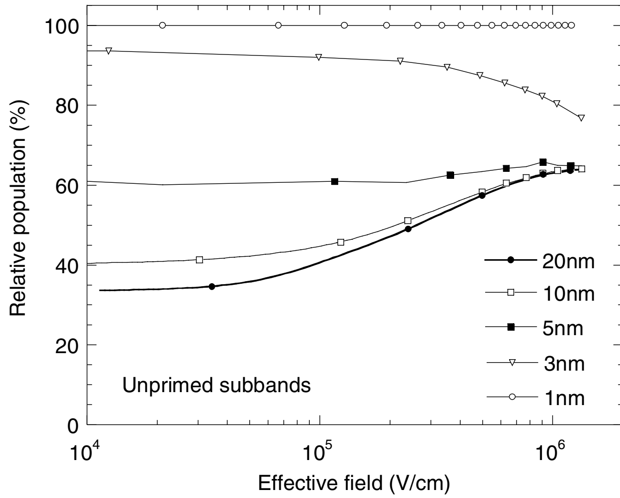

Figure 2. Relative population of unprimed subband versus the effective field for different film thicknesses.

with m_l perpendicular to the surface provide the lowest energy subband compared to the subbands associated with the four valleys whose mass m_t is lower than m_l. In a large range of E_{eff} and T_{SOI}, the electronic structure will evolve differently. Figure 1 illustrates the energy difference between the ground subband of the two ladders versus the transverse effective field. A high effective field leads to a steeper potential at the Si/SiO_2 interface which causes a more important splitting energy between unprimed and primed subbands. This effect is verified for ultrathin films. Indeed the energy difference between the primed subband and the unprimed subband ($E'_0 - E_0$) increases due to quantum confinement effects. As a consequence the relative population in the valleys will be modulated by both the transverse effective field and the silicon film thickness. This phenomenon has been well described in [8, 9].

Figure 2 exhibits the relative population of electrons in the unprimed subbands versus the effective field for various silicon film thicknesses T_{SOI}. For $T_{SOI} \geqslant 5$ nm, there is an increase of relative population when the silicon film thickness is reduced due to high values of energy difference between primed and

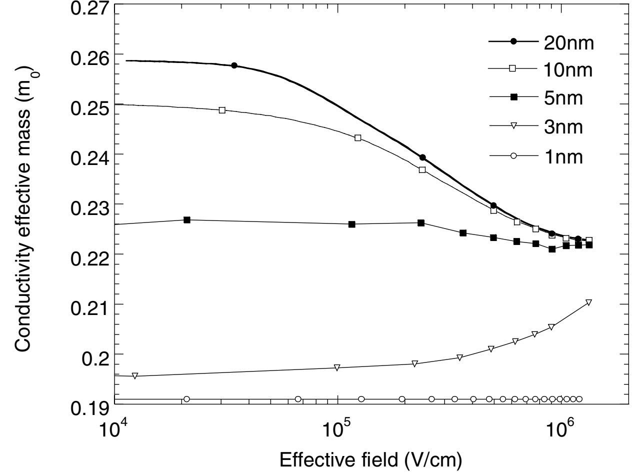

Figure 3. Evolution of the conductivity mass for different silicon film thicknesses.

unprimed subbands ($E'_0 - E_0$). This behaviour is slightly weakened at high E_{eff} for which the quantum confinement well at the Si/SiO_2 interface is more significant and yields higher values of $E'_0 - E_0$. For $T_{SOI} = 1$ nm, all electrons are located in the first unprimed subband. However, a slight reduction of the relative population versus E_{eff} is observed for $T_{SOI} = 3$ m. At low E_{eff} the energy level E'_0 is high and as observed for $T_{SOI} = 1$ nm nearly all electrons are in the unprimed subband. On the other hand, when E_{eff} increases, E'_0 gets closer to the Fermi level and authorizes an occupation of the primed subbands. It results in a slight reduction of the relative population of electrons located in the unprimed subbands as shown in figure 2. The relative population of the primed subband is not shown in this work but can be easily deduced. As a consequence of the subband modulation effect the conductivity effective mass also shows a dependence on both the silicon film thickness and the transverse effective field.

Figure 3 shows an important impact of the subband modulation on the conductivity mass for silicon film thicknesses ranging from 20 nm down to 1 nm. Consequently to the increase of the electron population in the unprimed valleys the conductivity mass decreases to attain m_t in ultrathin silicon film. It can be noted an opposite behaviour for $T_{SOI} = 3$ nm resulting from the relative population of electrons in the twofold valleys as described in figure 2. Another important effect in the calculation of the phonon-limited electron mobility is the form factor W_{ij} defined in equation (4). In figure 4 we show the dependence of W_{ij} for different thicknesses of silicon film and the two effective fields: $E_{eff} = 10^5$ and $E_{eff} = 10^6$ V cm^{-1}.

It results in a weak dependence on the thickness for T_{SOI} ranging from 40 nm down to 5 nm and in an important increase for T_{SOI} lower than 5 nm. The consequence of the decrease of the conductivity mass and the increase of the form factor for various silicon film thicknesses is observed on the phonon-limited electron mobility in figure 5. The mobility for electrons is calculated with equation (24) of [12]. A similar methodology has been applied for strained-silicon films with a 0.8% biaxial tensile strain (20% Ge equivalent strain). In this case all the carriers are located in the twofold valleys

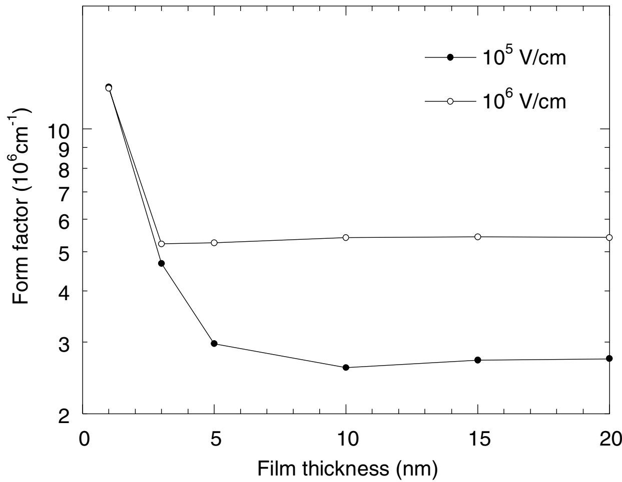

Figure 4. Evolution of the form factor W_{00} for the ground subbands as a function of the silicon thickness for two values of effective field (10^5 V cm^{-1} and 10^6 V cm^{-1}).

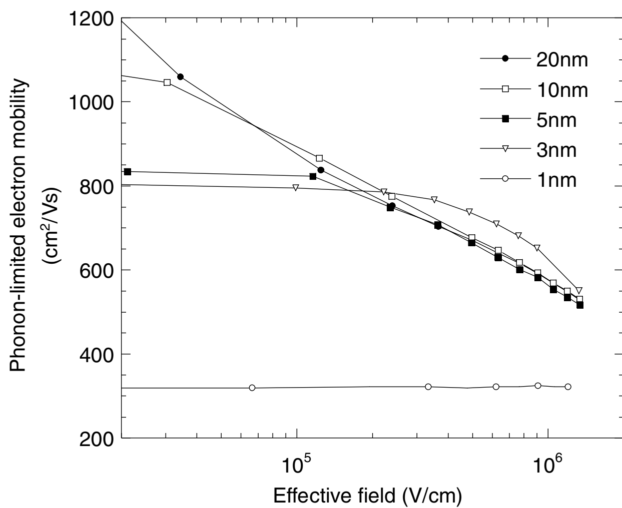

Figure 5. Theoretical phonon-limited electron mobility in a FD-SOI versus the transverse electric field for different thicknesses of a silicon film.

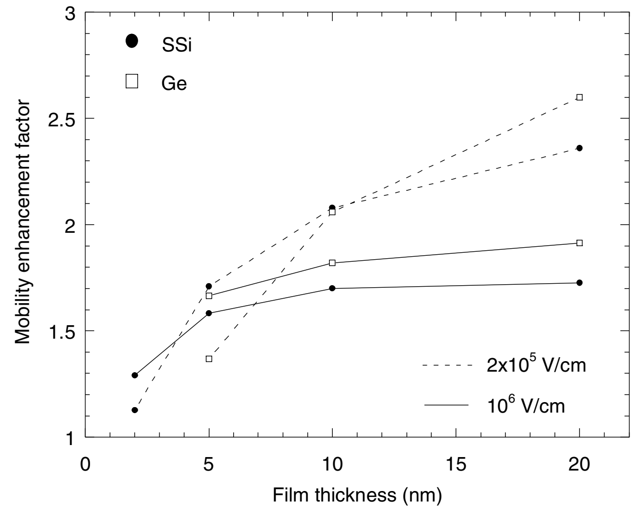

Figure 6. Enhancement factor of phonon-limited electron mobility in strained-Si and germanium with respect to Si mobility as a function of the film thickness.

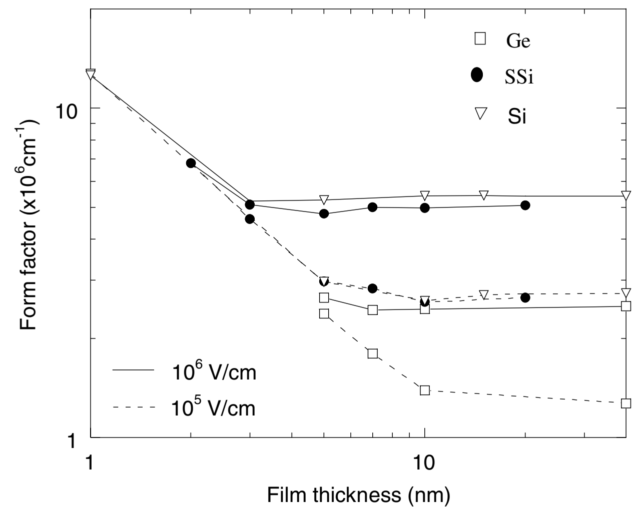

Figure 7. Evolution of the form factor W_{00} for the ground subbands as a function of the film thickness for $E_{eff} = 10^5$ V cm^{-1} and $E_{eff} = 10^6$ V cm^{-1}.

[12]. The different parameters used for the resolution of Poisson/Schrödinger equations and for the calculation of the mobility are listed in table 1. Figure 6 summarizes the enhancement factor of electron mobility defined by the ratio of mobility in strained-Si to that in unstrained-Si as a function of the semiconductor film thickness. A mobility enhancement of ∼2 is expected using sSi with $T_{sSOI} = 10$ nm.

The gain can be explained by a lower conductivity effective mass induced by the fact that all electrons are located in the twofold valleys. The form factor calculated in the strained silicon film which exhibits a similar behaviour compared to the unstrained silicon, i.e. an increase of W_{ij} when the film thickness decreases, is not sufficient to cancel out the effect of the reduced conductivity mass. Indeed with a 0.8% biaxial tensile strain, W_{ij} is close to the Si value (figure 7). It can be noted that the value of the form factor is all the more important as the effective field is high. The degradation of the enhancement factor for low thicknesses can be explained by the value of the conductivity mass in the unstrained silicon which tends to the value m_t (figure 3) and cancels out the strain effect.

The results obtained for the germanium are reported in figures 6 and 7. As for the strained silicon we observe an enhancement of mobility. At high electric field (10^6 V cm^{-1}) the enhancement factor follows the same trend as in sSi with a slightly improvement of mobility. On the other hand, at low transverse electric field (2×10^5 V cm^{-1}) we observe an inversion of the enhancement factor between sSi and Ge for a film thickness equal to 10 nm.

This effect can be explained in analysing the evolution of the form factor as a function of the film thickness (figure 7). For large thicknesses the form factor in Ge is much lower than in sSi which leads to higher mobilities in spite of a more important conductivity mass. By decreasing the film thickness to values lower than 10 nm we observed a Ge form factor which tends to the sSi value and the enhancement factor is inverted between sSi and Ge. We must not forget

that phonon scattering is not the only scattering mechanism present. Coulomb interaction and surface roughness may have a non-negligible influence in such thin devices and thus modify the gain of the phonon-limited electron mobility.

4. Conclusion

A comparative study of the phonon-limited electron mobility in ultrathin SOI, sSOI (0.8% biaxial tensile strain) and GeOI has been studied using a relaxation time approximation method. After having described the theoretical model we have demonstrated the important role played by quantization effects on the conductivity effective mass and on the form factor values. Through the evolution of these two physical parameters the mobility enhancement factor in sSi and Ge has been analysed at low and high transverse electric fields. A gain of mobility of $\sim$2 is obtained at $T_{SOI} = 10$ nm for both sSi and Ge materials.

References

[1] Taur Y 2002 *IBM J. Res. Devices* **46** 213–21

[2] Jaud M-A, Barraud S and Le Carval G 2004 *Proc. Nanotech2004* vol 2 pp 17–20

[3] Cassan E, Dollfus P, Galdin S and Hesto P 2001 *IEEE Trans. Electron. Devices* **48** 715–21

[4] Ramey M and Ferry D K 2003 *IEEE Trans. Nanotechnol.* **2** 193–7

[5] Dollfus P, Bournel A, Galdin S and Barraud S 2004 *IEEE Trans. Electron. Devices* **51** 749–56

[6] Frank D J, Dennard R H, Nowak E, Solomon P M, Taur Y and Wong H-S P 2001 *Proc. IEEE* **89** 259–87

[7] Wong H-S P 2002 *IBM J. Res. Devices* **46** 133–67

[8] Shoji M, Omura Y and Tomizawa M 1997 *J. Appl. Phys.* **81** 786–94

[9] Shoji M and Horiguchi S 1999 *J. Appl. Phys.* **85** 2722–31

[10] Gamiz F and Fischetti M V 2001 *J. Appl. Phys.* **89** 5478–87

[11] Lauer I *et al* 2004 *IEEE Electron. Device Lett.* **25** 83–5

[12] Takagi S-I, Hoyt J L, Welser J J and Gibbons J F 1996 *J. Appl. Phys.* **80** 1567–77

[13] Rieger M M and Vogl P 1993 *Phys. Rev.* B **48** 14276

[14] Fawcett W and Paige E G S 1971 *J. Phys. C: Solid State Phys.* **4** 1801–21

[15] Jayaraman A, Kosicki B and Irvin J C 1968 *Phys. Rev.* **171** 836–8

[16] Levinger B B and Frankl D R 1961 *J. Phys. Chem. Solids* **20** 281–8

[17] *Atlas User's Manual* 2002 vol 2, pp 12–4

[18] Koga J, Takagi S-I and Toriumi A 2002 *IEEE Trans. Electron. Devices* **49** 1042–8

[19] Ando T, Fowler B and Stern F 1982 *Rev. Mod. Phys.* **54** 437–672